Journal of King Saud University - Science 36 (2024) 103461

HOSTED BY

Contents lists available at ScienceDirect

Journal of King Saud University - Science

journal homepage: www.sciencedirect.com

# Synergistic antibacterial activity of biogenic AgNPs with antibiotics against multidrug resistant bacterial strains

Khalid Maniah [a], Fatimah Olyan Al-Otibi [a], Sara Mohamed [b,*], Basant A. Said [c], Mohamed Ragab AbdelGawwad [d], Mohamed Taha Yassin [a,*]

[a] Botany and Microbiology Department, College of Science, King Saud University, P.O. 2455, Riyadh 11451, Saudi Arabia
[b] Botany and Microbiology Department, Faculty of Science, Benha University, Benha 13511, Egypt
[c] Faculty of medicine, Cairo University, Cairo, Egypt
[d] Genetics and Bioengineering Department, Faculty of Engineering and Natural Sciences, International University of Sarajevo, 71210 Sarajevo, Bosnia and Herzegovina

ARTICLE INFO

*Keywords:*
Fenugreek
Seed extract
Drug resistance
Antibacterial
Synergism
Colistin
Norfloxacin

ABSTRACT

The prevalence of hospital-acquired infections caused by drug resistant bacterial pathogens is a major health risk, leading to a considerable number of deaths and illnesses globally. Therefore, it is essential to develop new combinations of antimicrobial agents to effectively manage drug-resistant bacteria that are responsible for nosocomial infections. A current study aims to synthesize silver nanoparticles (AgNPs) from the seeds of *Trigonella foenum-graecum* (fenugreek). The AgNPs exhibited a spherical morphology and had an average particle size of 29.75 nm. In addition, XRD examination verified the presence of a face-centered cubic (fcc) lattice structure in the biosynthesized AgNPs, while FTIR study demonstrated the existence of several functional groups such as phenols, alkanes, and amines. The biogenic AgNPs exhibited the most potent antibacterial effect against *E. coli* strain, with relative inhibitory zone of 18.43 ± 0.35 mm and a minimum inhibitory concentration (MIC) of 50 µg/ml. In addition, the most potent antibacterial effect of AgNPs combined with colistin was observed against *Acinetobacter baumannii* strain, while the greatest combined efficacy of AgNPs with norfloxacin was found against *Pseudomonas aeruginosa*, resulting in a relative increase in the fold of inhibition area (IFA) of 0.53 and 0.35, respectively. In conclusion, the potent antibacterial and synergistic effect of AgNPs with antibiotics highlights their potential application of this combination in controlling nosocomial infections in health care settings.

## 1. Introduction

Nanotechnology involves the crafting, synthesis, and manipulation of materials on a nanoscale to attain distinct properties that can be effectively utilized for specific applications (Bora et al., 2024). Recently, a broad spectrum of applications and emerging disciplines across various fields, including optics, chemical industries, mechanics, electronics, space industries, single electron transistors, light emitters, energy science, nonlinear optical devices, photoelectrochemical catalysis, biomedical cosmetics, drug or gene delivery, and food and feed, has extensively embraced the capabilities of nanotechnology (Dhaka et al., 2023). Particles with dimensions ranging from 1 to 100 nm, possessing at least one dimension within this scale, are termed nanoparticles (NPs) (Calzolai et al., 2012; Calderón-Jiménez et al., 2017). In recent times, Metallic nanoparticles (MNPs) have garnered significant attention due to their distinctive physicochemical features, high monodispersity and small size (Shnoudeh et al., 2019; Nie et al., 2023). In this context, AgNPs are synthesized by various techniques including physical, chemical and biological. Limitations of physical and chemical synthesis methods for synthesizing AgNPs include costly procedures and hazardous substances that might lead to potential environmental and biological risks (Kakakhel et al., 2021). Hence, it was necessary to develop techniques to address these constraints and synthesize durable and pharmacologically effective AgNPs (Syafiuddin et al., 2017b). Nanoparticles are produced using various biological components such as plant extracts and microorganisms. The biological extract contains amino acids, proteins, vitamins, polysaccharides, enzymes, and phytoconstituents that function as reducing agents (Polash et al., 2021; Hamad et al., 2020). *Trigonella foenum-graecum* (L.), generally known as Fenugreek, is a fragrant leguminous plant cultivated in several countries. Fenugreek seeds have traditionally been used for their medicinal abilities to cure arthritis, diabetes, gastrointestinal issues, as well as for their anti-

* Corresponding authors at: Botany and Microbiology Department, Faculty of Science, Benha University, Benha 13511, Egypt.
*E-mail addresses:* sara.m.elsayed@gmail.com (S. Mohamed), myassin2.c@ksu.edu.sa (M. Taha Yassin).

https://doi.org/10.1016/j.jksus.2024.103461
Received 5 May 2024; Received in revised form 18 September 2024; Accepted 19 September 2024
Available online 21 September 2024

parasitic and anticancer characteristics (Awad et al., 2021). Previous studies reported the synergistic antibacterial activity of AgNPs with antibiotic as fosfomycin (Aljeldah et al., 2023), colistin (Yassin et al., 2022a), tigecycline, and linezolid (Al-Otibi et al., 2023). Prior research emphasized the eco-friendly production of biogenic silver nanoparticles using plant seed extracts, but few studies investigated the combined effect of these nanoparticles with antibiotics. The research aimed to assess the antimicrobial and combined effects of the eco-friendly synthesized AgNPs with norfloxacin and colistin antibiotics against multidrug-resistant bacterial strains. The fabricated AgNPs were synthesized using seed extract of *Trigonella foenum-graecum* and their combined activities with colistin and norfloxacin antibiotics were evaluated against multidrug–resistant gram negative bacterial strains namely, *Acinetobacter baumannii, Klebsiella pneumoniae, Pseudomonas aeruginosa* and *Escherichia coli* strains.

## 2. Materials and methods

### 2.1. Preparation of Fenugreek seed extract

The seeds of Fenugreek were procured from a Riyadh, Saudi Arabian market, and the Herbarium of King Saud University's College of Science verified their authenticity. After being washed with tap water, the seeds were rinsed three times with distilled water for a complete cleaning procedure. They were then left to air dry. To make a fine powder out of the Fenugreek seeds, a mechanical mortar was used. After that, 50 g of powder were dissolved in 200 ml of distilled water, and the mixture was then heated in flasks at 50 °C for half an hour. The subsequent mixture was agitated with a magnetic stirrer for 24 h at 25 °C. To get a clear filtrate, the Fenugreek seeds extract was next filtered using Whatman filter paper (1). The extract was sterilized by passing it through a 0.45 μm Millipore membrane filter, and then it was stored in the fridge at 4 °C until later use.

### 2.2. Green synthesis of AgNPs

Initially, 10 mL of the water extract obtained from Fenugreek seeds was added to 90 mL of a 1 mM solution of colorless $AgNO_3$ (Sigma-Aldrich, Missouri, USA). Subsequently, 90 mL of silver nitrate solution was mixed with 2, 4, 6, 8, and 10 mL of Fenugreek seed extract, each at a silver nitrate concentration of 1 mM. Additionally, different concentrations of $AgNO_3$ (0.2, 0.4, 0.6, 0.8, and 1.0 mM) were used to synthesize silver nanoparticles while maintaining a constant extract concentration (2 mL).

Subsequently, the reaction mixture underwent incubation at room temperature in a shaking incubator under dark conditions. The biosynthesis process of AgNPs was visually monitored, observing a color shift from colorless to a light brown hue. AgNPs were separated from the reduced mixture through centrifugation at 10,000 rpm for 10 min. The collected AgNPs underwent a thorough washing process with deionized water, repeated three times to eliminate impurities. Subsequently, the extract underwent sterilization through filtration, employing a Millipore membrane filter with a pore size of 0.45 μm. Finally, the purified AgNPs were dried at 80℃ in an oven for subsequent physicochemical characterizations (Yassin et al., 2022b, 2022c).

### 2.3. Physicochemical properties of the biogenic AgNPs

The physicochemical features of the biogenically synthesized AgNPs were explored through diverse methodologies as UV–Vis, TEM, EDX, FTIR, XRD and zeta potential analysis of the biosynthesized AgNPs.

### 2.4. Screening of antimicrobial efficacy of AgNPs against bacterial pathogens

The American Type Culture Collection provided four bacterial strains: *A. baumannii* (ATCC 43498), *K. pneumoniae* (ATCC 700603), *E. coli* (ATCC 25922), and *P. aeruginosa* (ATCC 9027). The selection of bacterial pathogens for antimicrobial investigations was based on their substantial impact on worldwide mortality and morbidity, which is mostly caused by their extensive antibiotic resistance. The antibacterial efficacy of biogenic AgNPs was examined against the identified bacterial strains using the disc diffusion technique. The bacterial colonies were collected, mixed with a saline solution, and adjusted to a concentration of $10^8$ cfu/mL using the 0.5 McFarland standard. After filling sterile Petri plates with sterile Mueller Hinton agar (MHA) media and inoculating them with the bacterial solution, 8 mm filter paper discs impregnated with 100 and 200 μg of AgNPs were added. Filter paper discs soaked with methanol solvent functioned as the negative controls, and Colistin sulfate as the positive control. Plates were incubated at 37 °C for 24 h after being refrigerated for 2 h to facilitate the diffusion of nanoparticles. A Vernier caliper was used to measure the inhibitory zone diameters. The broth microdilution test employing 96-well microtiter plates was used to evaluate the minimum inhibitory concentration (MIC) of AgNPs from Fenugreek seeds against the most sensitive strain of *E. coli*. In addition, the minimum bactericidal concentration (MBC) was determined by inoculating samples from MIC wells onto MHA plates. The MBC was defined as the lowest concentration at which no bacterial growth was observed.

### 2.5. Determination of synergistic potency of biogenic AgNPs with antibiotics

The combined efficacy of antibiotic-AgNPs against certain bacterial pathogens was evaluated via the use of disc diffusion assay. Fresh MHA plates were made and then inoculated with 0.5 mL of the bacterial solution that was prepared earlier. A separate set of discs was impregnated with both of colistin (10 μg) or norfloxacin (10 μg) and AgNPs (100 μg/disk) to examine their synergistic effect. The positive control discs were loaded with colistin (10 μg) and norfloxacin (10 μg) only, whereas the negative control discs were filled with filter paper discs soaked in methanol solvent. The moistened discs were allowed to dry before being positioned on the MHA plates that had been previously inoculated. Following that, the dishes were subjected to incubation at a temperature of 37 ℃ for a period of 24 h. The calculation of the increase in fold of inhibition area (IFA) was performed utilizing the subsequent equation:

$(IFA) = (B^2 - A^2)/A^2$, where A was the diameter of the inhibition zone for colistin or norfloxacin antibiotics and B was the diameter of the inhibition zone for antibiotics and biogenic AgNPs combined together (Al-Otibi et al., 2023).

### 2.6. Determination of morphological cell deformations

Scanning electron microscopy (SEM) was utilized to assess the morphological changes in bacterial cells treated with biosynthesized AgNPs. The samples were processed for investigation as mentioned in a prior study (Almaary et al., 2023).

## 3. Results and discussion

### 3.1. Optimization of the reaction conditions

Various volumes of the plant extract and varying concentrations of $AgNO_3$ were examined to determine the factors that contribute to achieving the highest yield of AgNPs. In this context, it was seen that the highest amount of AgNPs was produced when using a concentration of 1 mM of $AgNO_3$ and 10 ml of the plant extract. This resulted in the development of AgNPs precipitates with concentrations of $0.57 \pm 0.04$ and $1.47 \pm 0.09$ mg/ml, respectively (Fig. 1).

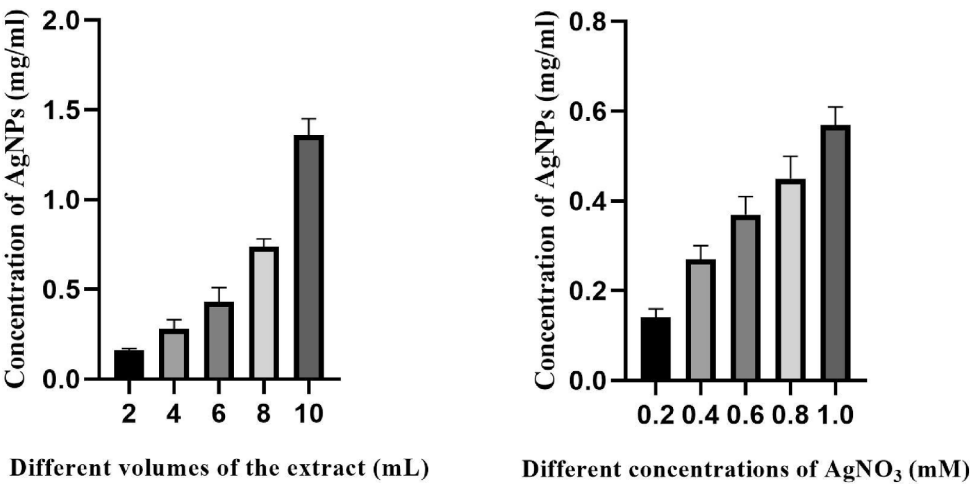


**Fig. 1.** Effect of different concentrations of $AgNO_3$ and plant extract on the yield of AgNPs.

### 3.2. Green synthesis of AgNPs

Fig. 2 showed the green fabrication of AgNPs using seed extract of Fenugreek. The colorless solution of silver nitrate (Fig. 2a) undergoes reduction when mixed with the liquid extract of Fenugreek seeds, leading to the creation of silver nanoparticles. The Fenugreek seeds include a variety of natural chemical components, including amino acids, flavonoids, saponins, alkaloids, and steroids. These components are responsible for the extensive usage of seed extracts in the environmentally friendly production of various metal and metal oxide nanoparticles (Jeevanandam et al., 2022). Furthermore, the extract phytochemicals function as capping and stabilizing agents, playing an important role in the production of AgNPs (Restrepo and Villa, 2021).

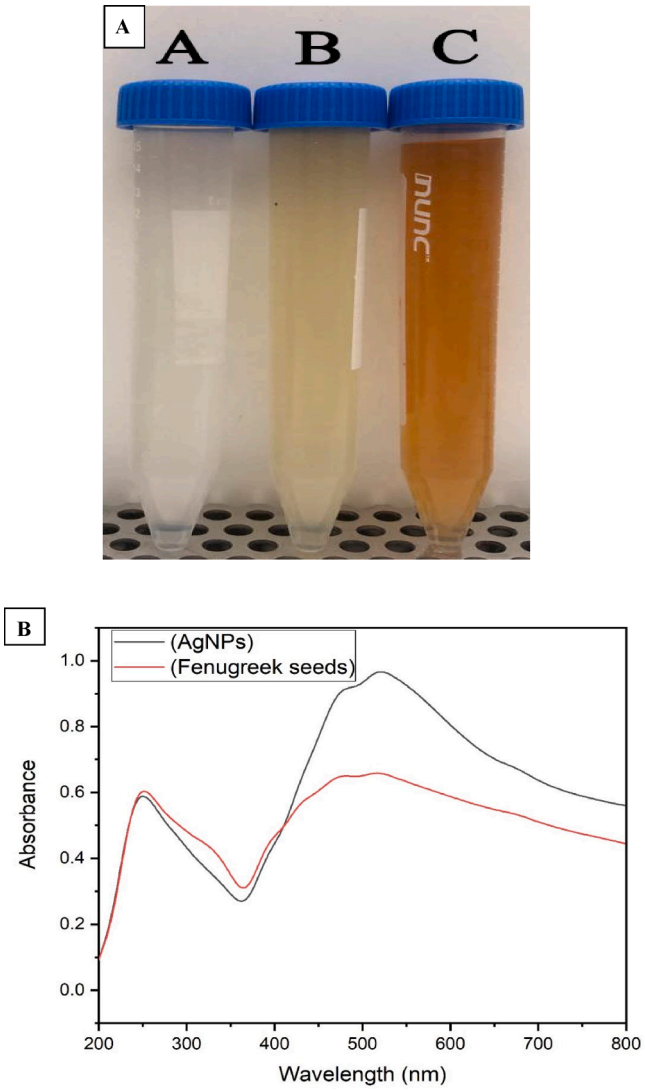


**Fig. 2.** a) Green synthesis of AgNPs using *T. foenum-graecum* seeds extract, b) UV spectrum of Fenugreek seeds extract and their corresponding AgNPs.

### 3.3. UV analysis of biogenic AgNPs and Fenugreek seed extract

The surface plasmon resonance (SPR) of the biosynthesized AgNPs was determined by analysing the Fenugreek seed extract and AgNPs with UV analysis. The coordinated motion of electrons within the conduction band of nanoparticles upon absorption of an electromagnetic wave is referred to as surface plasmon resonance. In this setting, Fenugreek extract shown the existence of two absorption bands at 251 and 507 nm. Consistent with the outcomes of a prior study, our results confirmed the presence of a distinctive peak at 500 nm in the UV spectrum of the water extract of red currant (Rizwana et al., 2022). The absorption behavior seen in Fig. 2b is caused by SPR of AgNPs, which occurs when conduction band electrons of the AgNPs undergo coherent oscillation in response to the electromagnetic field. This explains the presence of a broad band with distinctive peaks at 476 and 509 nm in the UV spectrum of plant extract, which were shifted to a higher wavelength in the UV spectrum of AgNPs at 480 and 519 nm. The results of our study were consistent with those of a prior publication (Syafiuddin et al., 2017a).

### 3.4. TEM analysis of AgNPs

TEM micrographs of AgNPs showed that the nanoparticles were spherical in shape with average particle size of 29.75 nm (Fig. 3a). The histogram of the particle size distribution indicated that the size of the AgNPs varied between 10 and 70 nm (Fig. 3b). The findings of our study aligned with a previous publication that showed the successful production of silver nanoparticles (AgNPs) using olive leaf extract. The report reported that the average particle size of the AgNPs was around 30 nm (Khalil et al., 2014). Additionally, another research used transmission electron microscopy (TEM) to analyze AgNPs morphology made from an aqueous leaf extract of *Azadirachta indica*. According to the research, these AgNPs had an average size of 34 nm (Ahmed et al., 2016). The measured particle size was smaller than in earlier

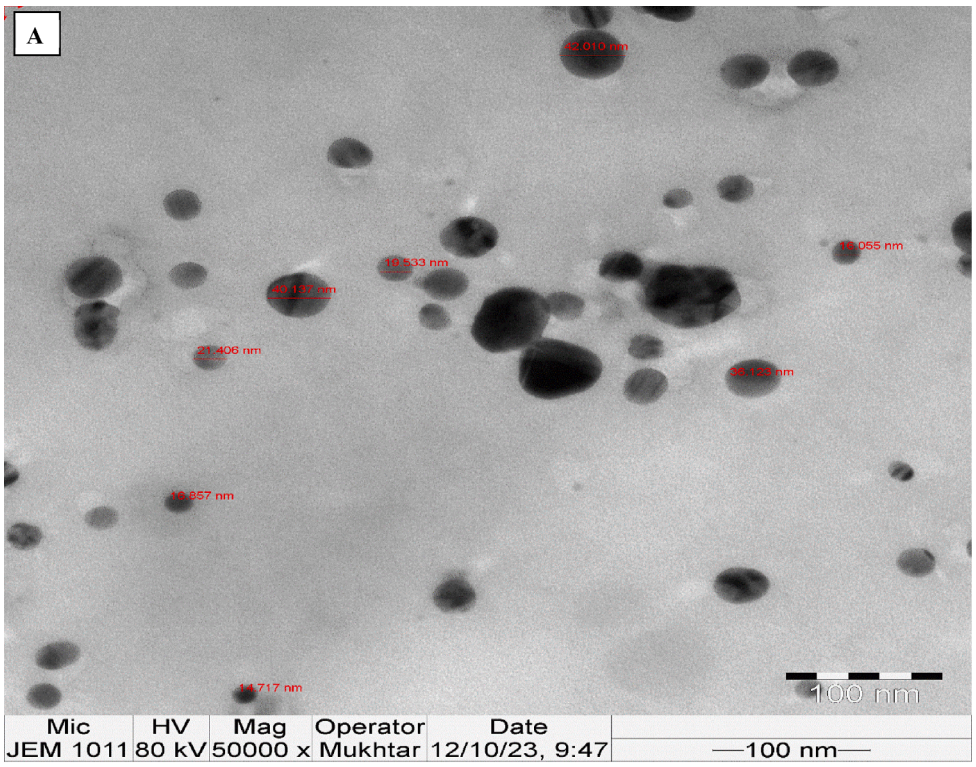


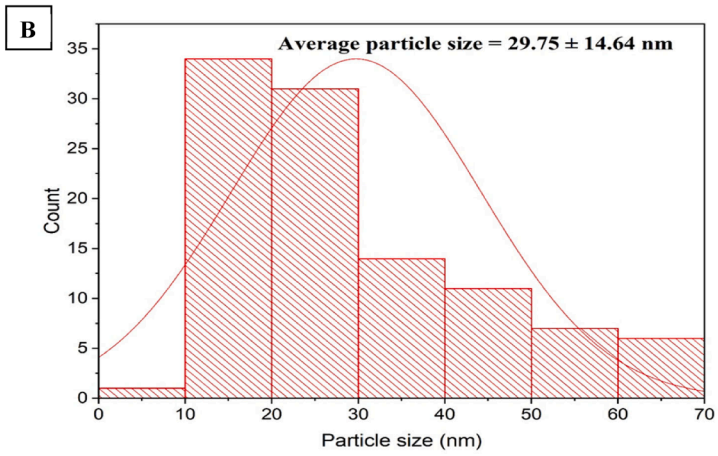


**Fig. 3.** A) tem images of agnps, b). particle size distribution of agnps.

publications, showing the effectiveness of the present approach for synthesizing AgNPs using the seed extract of *T. foenum-graecum*.

### 3.5. EDX analysis of the biogenic AgNPs

EDX analysis was used to conduct elemental mapping of the biogenic AgNPs (Fig. 4a). The study revealed that the proportion of elemental silver was 73.42 %, whereas the percentage of oxygen was 26.58 %. The strong signals at 2.983 keV were attributed to silver atoms, whereas the signal at 0.525 keV was allocated to oxygen atoms. The mass percentage of elemental Ag was more than that reported in a recent work on the green synthesis of AgNPs using the endophytic fungus *Talaromyces purpureogenus*, which was isolated from *Taxus baccata* Linn. The relative mass percentage was found to be 67.26 % (Sharma et al., 2022). Additionally, the EDX examination revealed that the AgNPs synthesized utilizing leaf extract of *Holoptelea integrifolia* had an elemental content of 71.32 % Ag (Kumar et al., 2019).

### 3.6. FTIR analysis of the biogenic AgNPs

FTIR investigation of Fenugreek seed extract and AgNPs was done to detect the key functional groups contributing to the reduction, capping and stabilizing of AgNPs. In this setting, FTIR spectrum of the seed extract of Fenugreek displayed the existence of six peaks at 3395.87, 2081.10, 1637.88, 1386.34, 1115.38, and 662.29 $cm^{-1}$ (Fig. 4b). On the other hand, the FTIR spectrum of AgNPs displayed the existence of nine absorption bands at wavenumbers of 3416.42, 2926.18, 2370.75, 2047.32, 1628.06, 1388.77, 1114.91, 619.97 and 477.98 $cm^{-1}$. The wide spectral band observed at 3395.87 $cm^{-1}$ in the Fenugreek spectrum was identified as the result of O–H stretching of phenolic

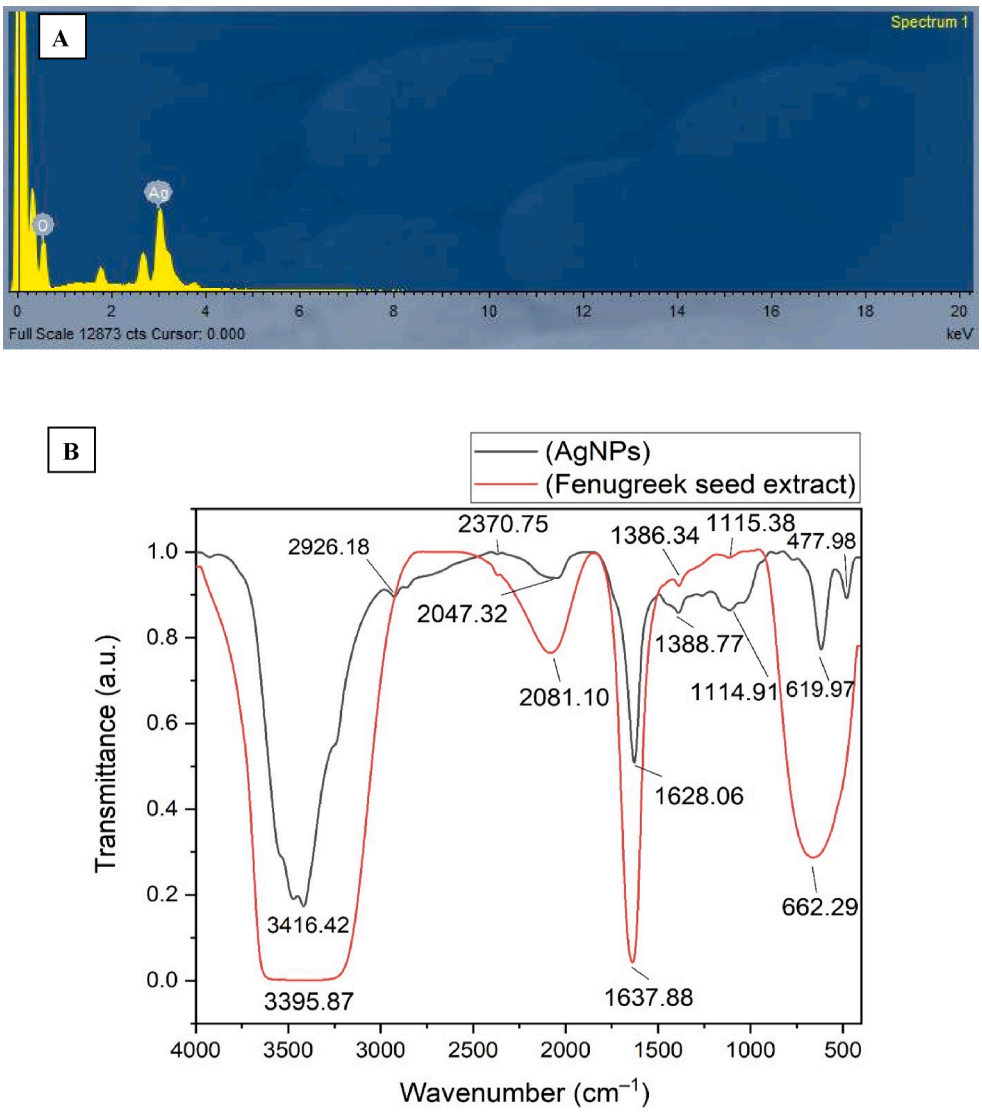


**Fig. 4.** A) edx spectrum of agnps (x axis refereed to the energy level (kev) whereas y axis refer to the counts), b) FTIR spectrum of Fenugreek seeds extract and AgNPs.

biomolecules. In AgNPs spectrum, this peak was shifted to a higher wavenumber at 3416.42 $cm^{-1}$, indicating that the extract phenols were adsorbed over nanoparticles surface (Hajebi et al., 2019). The spectra of AgNPs displayed two weak bands with wavenumbers of 2926.18 and 2370.75 $cm^{-1}$. These peaks were identified as the result of stretching vibrations of C–H and N–H bonds in alkanes and amines, respectively (Oves et al., 2022). In contrast, the peak seen at 2081.10 $cm^{-1}$ in the seed extract was shifted to a lower wavelength at 2047.32 $cm^{-1}$, these bands were attributed to the C=S stretching of sulfur compounds (Mistry et al., 2021). Moreover, the absorption band seen at 1637.88 $cm^{-1}$ in spectra of Fenugreek seed extract was shifted to a lower wavenumber at 1628.06 $cm^{-1}$, corresponding to the amide I bands of proteins (Das et al., 2013). The peak seen at 1388.77 $cm^{-1}$ in the spectra of AgNPs was displaced to a lower wavenumber of 1386.34 $cm^{-1}$, indicating the C–H bending of alkanes. Nevertheless, the peak detected at 1114.91 $cm^{-1}$ in the Fenugreek seed extract spectra was displaced to a higher frequency at 1115.38 $cm^{-1}$ in the AgNPs spectra, indicating the C-N stretching of amines (Deivanathan and Prakash, 2022). The strong peak detected at 662.29 $cm^{-1}$ was shifted to a lower wavenumber at 619.97 $cm^{-1}$ corresponding to S-S stretching (Raghava et al., 2021).

### 3.7. XRD analysis of AgNPs

XRD investigation was performed to affirm the crystalline structure of the eco-friendly synthesized AgNPs. XRD analysis showcased the existence of six diffraction peaks at 2 theta angles of 21.19, 32.28, 37.31, 49.34, 57.48 and 77.55° corresponding to the orientation planes of (1 0 0), (1 1 0), (1 1 1), (2 0 0), (2 2 0) and (3 1 1), respectively (Fig. 5). The XRD outcomes were in line with that of previous reports (Varghese et al., 2019). The detected peaks validate the polycrystalline characteristic of the synthesized AgNPs and may be ascribed to the typical JCPDS data of crystalline silver with a face-centered cubic (fcc) lattice structure, identified by the code COD 2300113. The additional peaks seen in XRD pattern correspond to the organic stabilizers that inhibit the aggregation of AgNPs (Jalilian et al., 2020). The bioprepared AgNPs were found to have a crystalline size of 28.71 nm, which was determined using Scherrer's equation.

The formula for calculating the crystalline size is given by $D=0.9\lambda/\beta\cos\theta$, where $\lambda$ represents the X-ray wavelength (1.54178 Å), k represents Scherrer's constant ($k = 0.94$), $\theta$ represents the diffraction angle (32.31°), and $\beta$ represents the full width at half maximum (FWHM) of the most intense diffraction peak (0.301) (Yassin et al., 2023). The physicochemical features of the biogenic AgNPs were compared with

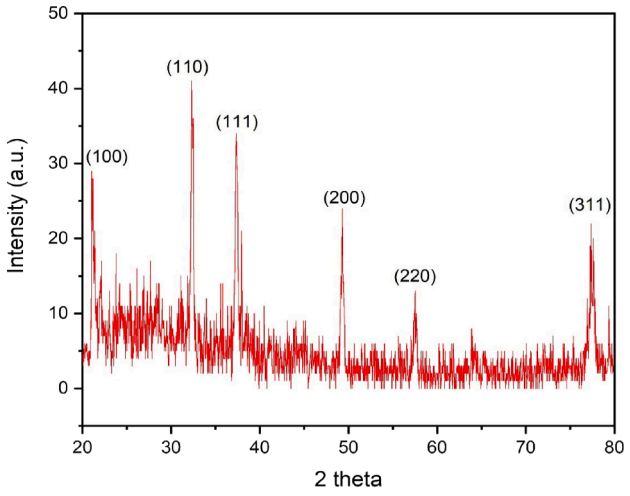


**Fig. 5.** XRD spectrum of AgNPs.

that of previous literature as seen in Table 1.

### 3.8. Zeta potential analysis

Zeta potential analysis was done to estimate the zeta potential value of the eco-friendly synthesized AgNPs. The presence of high negative values suggests that anionic stabilizing agents are effectively coordinating with the AgNPs, resulting in a stable colloidal solution. This stability is achieved by the electrostatic repulsion between the negatively charged particles. The presence of negatively charged surfaces on AgNPs serves to inhibit the aggregation of nanoparticles and exert control over their shapes and sizes (Paosen et al., 2017). In this context, zeta potential value of AgNPs was detected to be –22.4 mV (Fig. 6a). However, the results from DLS displayed that the mean hydrodynamic nanosize of AgNPs was 166.9 nm (Fig. 6b). This size is larger than what was observed using TEM and XRD techniques. The difference might be accredited to the existence of capping biomolecules and the fact that DLS analysis measures both the nanoparticles diameter and the surrounding hydrate layers. The polydispersity index (PDI) of the biogenic AgNPs was estimated to be 0.364, which in agreement with the findings of a prior investigation that reported a PDI value of 0.365 for AgNPs synthesized using *Ginkgo biloba* leaf extract (Wang et al., 2019). This indicates that the synthesized AgNPs were effectively dispersed in water.

### 3.9. Antibacterial efficacy of AgNPs against the concerned microbial strains

The antibacterial efficacy of AgNPs was detected against *A. baumannii*, *E. coli*, *K. pneumoniae*, and MRSA pathogens using a disc diffusion assay. *E. coli* strain showed the highest antibacterial susceptibility to the biogenic AgNPs at the two tested concentrations of AgNPs (50 and 100 µg/disc), demonstrating relative suppressive zones of 18.43 ± 0.35 and 21.32 ± 0.19 mm, respectively (Table 2). Nevertheless, the *MRSA* strain exhibited the least sensitivity to the biogenic AgNPs at the tested doses, resulting in inhibitory zones of 10.24 ± 0.21 and 11.26 ± 0.51 mm, respectively. The study findings demonstrated that AgNPs exhibit greater antibacterial efficacy against Gram-negative bacteria compared to Gram-positive bacteria due to the presence of a peptidoglycan layer in the cell wall of Gram-positive bacteria (Ramalingam et al., 2016). This layer, consisting of glycan strands cross-linked by short peptides and anionic glycopolymers known as teichoic acid, acts as a natural barrier that hinders the penetration of nanoparticles. In contrast, Gram-negative bacteria possess a cell wall that is thinner and has a lower amount of peptidoglycan. Although lipopolysaccharides (LPS), a crucial element of the Gram-negative bacterial cell wall, greatly enhances the strength and integrity of the membrane, its negative charge promotes the attachment of nanoparticles (Tavares et al., 2020). Previous research has shown that reactive oxygen species (ROS) play a significant role in the antibacterial action of biosynthesized AgNPs, as shown in an evaluation of AgNPs' ROS-mediated antibacterial activity against multidrug-resistant *E. coli* and *S. aureus*. Consequently, the elevated amount of ROS caused the bacterial membranes to be disrupted by increasing their permeability. This ultimately led to the disruption of the electron transport chain and the leaking of cellular content, leading to the bacterial cell death (Das et al., 2017). The minimum inhibitory concentration (MIC) and minimum bactericidal concentration (MBC) were detected for *E. coli* strain which showed the highest sensitivity to AgNPs. The detected MIC and MBC values were found to be 50 and 100 µg/ml, respectively. The antimicrobial activity of AgNPs could be assigned to the capping agents adsorbed over the biogenic AgNPs as phenols, alkanes, amines, amide I bands of proteins, and alkanes as

**Table 1**
Comparison of the experimental results with previous literature.

| Plants | Functional groups of AgNPs | Crystalline size | Antibacterial activity | References |
|---|---|---|---|---|
| *Trigonella foenum-graecum* seeds extract | Phenols, alkanes, amines, amide I bands of proteins, alkanes, and sulfur compounds | 28 nm | Antibacterial activity against *A. baumannii, E. coli, K. pneumoniae,* and *P. aeruginosa* | This work |
| *Datura stramonium* leaf extract | Alcohols, phenols, carboxylic acids, proteins and aromatic compounds | 18 nm | Antibacterial activity against *E. coli and S. aureus* | (Gomathi et al., 2017) |
| *Croton sparsiflorus morong* leaf extract | Amines, alcohols, ketones, aldehydes and carboxylic acids | 16 nm | Antibacterial activity against *S. aureus, E. coli,* and *B. substilis* | (Kathiravan et al., 2015) |
| *Pedalium murex* leaf extract | Phenols, flavanones proteins, alkyl groups, aromatic and carboxylic compounds | 14 nm | Antibacterial activity against *E. coli, K. pneumoniae, B. subtilis and S. aureus* | (Anandalakshmi et al., 2016) |
| *Sesbania grandiflora* leaf extract | Amines, alcohols, ketones and carboxylic acid. | ND | Antibacterial activity against *S. enterica* and *S. aureus* | (Das et al., 2013) |
| *Fumaria officinalis* aerial plant extract | Alcohols, phenols, amines, amides, peptides and proteins | 20 nm | Antibacterial activity against gram positive bacteria *as S. aureus, B. cereus, B. luteus,* and *L. monocytogenes*; also against gram negative bacteria as *E. coli, P. aeruginosa, K. pneumoniae* and *P. vulgaris* | (Milorad Cakić et al., 2018) |
| *P. nigrum* leaf and stem extract | For leaf derived AgNPs: Ketones, secondary amines, nitro groups, esters, alkynes<br>For stem derived AgNPs: primary alcohols, primary and secondary amines, nitrile groups, and amides | 27 nm and 13.5 nm, respectively | Antibacterial activity against *Citrobacter freundii*and *Erwinia cacticida* | (Paulkumar et al., 2014) |
| *Syngonium podophyllum* leaf extract | Amide II, protein, secondary amine, and aldehydes | ND | Antibacterial activity against *S. aureus, B. subtilis, E. coli* and *P. aeruginosa* | (Naaz et al., 2021) |

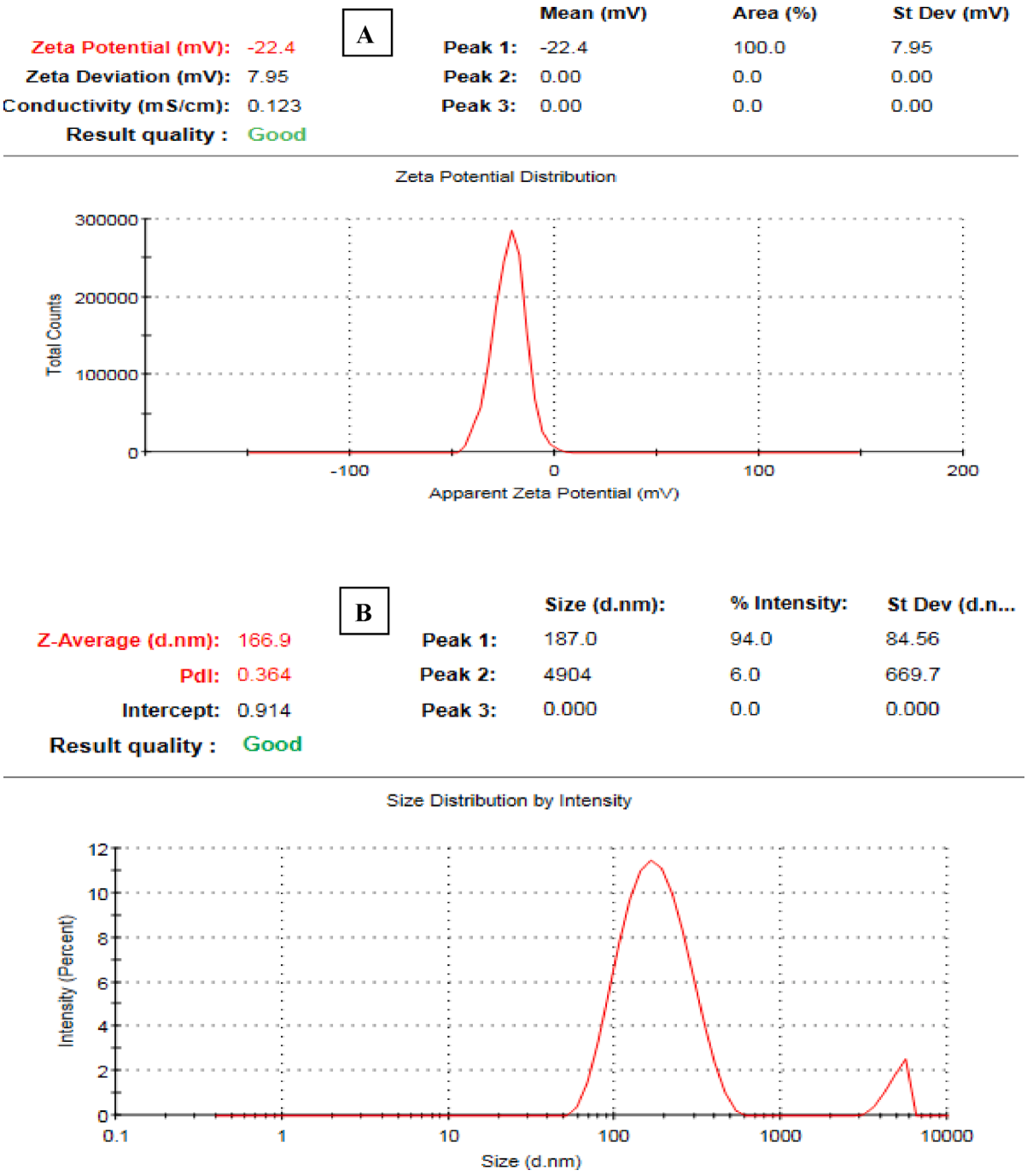


**Fig. 6.** A) zeta potential value of agnps, b) DLS spectrum of AgNPs.

detected by FTIR analysis and this was in accordance with previous report (Roy et al., 2019).

### 3.10. *Synergistic antibacterial efficiency of AgNPs with antibiotics*

The AgNPs exposed the uppermost synergistic efficacy with colistin against *A. baumannii* strain with relative IFA of 0.53 whereas AgNPs displayed the highest synergistic proficiency with norfloxacin against *P. aeruginosa* with relative IFA value of 0.35 (Table 3). Our outcomes were in line with that of a prior investigation which reported the antimicrobial action of silver nanoparticles conjugated with colistin against *E. coli*, *K. pneumoniae*, and *P. aeruginosa* (Muenraya et al., 2022). The combined action of AgNPs and colistin antibiotic against the gram negative bacterial strains is due to the impact of colistin antibiotic on the lipopolysaccharide, a key component of the outer membrane. This leads to the disruption of the outer membrane, allowing AgNPs to enter the bacterial cells. AgNPs then exert their killing effect by producing reactive oxygen species, that oxidize the bacterial DNA, proteins and lipids, ultimately resulting in the demise of the bacterial cells (Tripathi and Goshisht, 2022). An earlier work documented the synergistic effect of norfloxacin and gallotannin-capped iron oxide nanoparticles, showing an increase in inhibitory zones from 13 mm to 17 mm and 19 mm against the two strains, respectively (Ahmed et al., 2021). The combined effect of AgNPs and norfloxacin might be accredited to AgNPs accumulation on the outer membrane of bacterial cells, triggering their disruption. On the other hand, norfloxacin antibiotic inhibits bacterial growth by interacting with bacterial topoisomerase IV and DNA gyrase, thereby preventing DNA replication (Huang et al., 2024).

**Table 2**
Antibacterial efficiency of AgNPs against the concerned bacterial pathogens.

| Bacterial strains | AgNPs (50 µg/disk) | AgNPs (100 µg/disk) | Colistin (10 µg/disk) | Negative control |
|---|---|---|---|---|
| *A. baumannii* | 12.19 ± 0.21 [a] | 13.83 ± 0.14 [a] | 14.02 ± 0.32 [a] | 0.00 ± 0.00 |
| *E. coli* | 18.43 ± 0.35[b] | 21.32 ± 0.19[b] | 27.35 ± 0.29[b] | 0.00 ± 0.00 |
| *K. pneumoniae* | 14.52 ± 0.43[c] | 20.76 ± 0.31[b] | 21.05 ± 0.41[c] | 0.00 ± 0.00 |
| *P. aeruginosa* | 10.24 ± 0.21[c] | 11.26 ± 0.51[c] | 16.12 ± 0.24 [a] | 0.00 ± 0.00 |

Different superscript letters indicated that values were significantly different at $p \leq 0.05$.

**Table 3**
Synergistic antibacterial activity of AgNPs with antibiotics against drug resistant strains.

| Bacterial strains | AgNPs (100 µg/disk) + Colistin (10 µg/disk) | Colistin (10 µg/disk) | Negative control | IFA |
|---|---|---|---|---|
| *A. baumannii* | 20.27 ± 0.58 [a] | 13.89 ± 0.52 [a] | 0.00 ± 0.00 | 0.53 |
| *E. coli* | 34.94 ± 0.39[b] | 25.18 ± 0.26[b] | 0.00 ± 0.00 | 0.48 |
| *K. pneumoniae* | 27.18 ± 0.42[c] | 20.52 ± 0.48[c] | 0.00 ± 0.00 | 0.43 |
| *P. aeruginosa* | 19.16 ± 0.53 [d] | 16.43 ± 0.18 [d] | 0.00 ± 0.00 | 0.29 |
| | AgNPs (100 µg/disk) + norfloxacin (10 µg/disk) | norfloxacin (10 µg/disk) | Negative control | IFA |
| *A. baumannii* | 11.83 ± 0.18 [a] | 9.74 ± 0.26 [a] | 0.00 ± 0.00 | 0.32 |
| *E. coli* | 32.65 ± 0.18[b] | 28.79 ± 0.58[b] | 0.00 ± 0.00 | 0.22 |
| *K. pneumoniae* | 30.47 ± 0.29[c] | 24.96 ± 0.47[c] | 0.00 ± 0.00 | 0.33 |
| *P. aeruginosa* | 27.13 ± 0.41 [d] | 21.85 ± 0.34 [d] | 0.00 ± 0.00 | 0.35 |

IFA refers to increase in fold of inhibition area.
Different superscript letters indicated that values were significantly different at $p \leq 0.05$.

### 3.11. Detection of bacterial cell deformations using SEM analysis

The morphological deformations of *E. coli* cells were investigated using SEM analysis. The control cells of *E. coli* were found to be normal, rod-shaped, and with structural integrity without any signs of deformation. Moreover, it was observed that *E. coli* cells subjected to AgNPs treatment exhibited aberrant morphological characteristics, including cellular damage, wrinkling, malformation, as well as a cracked outer surface and distorted cell membranes (Fig. 7).

## 4. Conclusions

*Trigonella foenum-graecum* facilitated green biosynthesis of AgNPs with potential physicochemical techniques. The eco-friendly synthesized AgNPs were spherical in shape with mean nanosize of 29.75 nm and average zeta potential of –22.7 mV. Hence, the prepared AgNPs showed effective antimicrobial action against the concerned bacterial strains due to the potential physicochemical features of AgNPs such as the small particles size and the capping of biomolecules as phenols, alkanes and amines. The biogenic AgNPs showed a higher synergistic activity with colistin compared to norfloxacin antibiotic. The recorded synergistic activity of AgNPs with antibiotics highlights the potential use of these combinations to control nosocomial infections in health care settings. Moreover, the effective combination of AgNPs with colistin and norfloxacin antibiotics could offer potential therapeutic options against the drug resistant bacterial pathogens.

## Funding

This research project was supported by a grant from the Researchers Supporting Project number (RSP2024R114), King Saud University, Riyadh, Saudi Arabia.

## CRediT authorship contribution statement

**Khalid Maniah:** Software, Resources, Investigation, Formal analysis, Data curation. **Fatimah Olyan Al-Otibi:** Writing – review & editing, Writing – original draft, Validation, Supervision, Software, Resources. **Sara Mohamed:** Visualization, Software, Investigation, Formal analysis, Data curation. **Basant A. Said:** Software, Methodology. **Mohamed Ragab AbdelGawwad:** Writing – review & editing. **Mohamed Taha Yassin:** Writing – review & editing, Writing – original draft, Supervision, Project administration, Methodology,

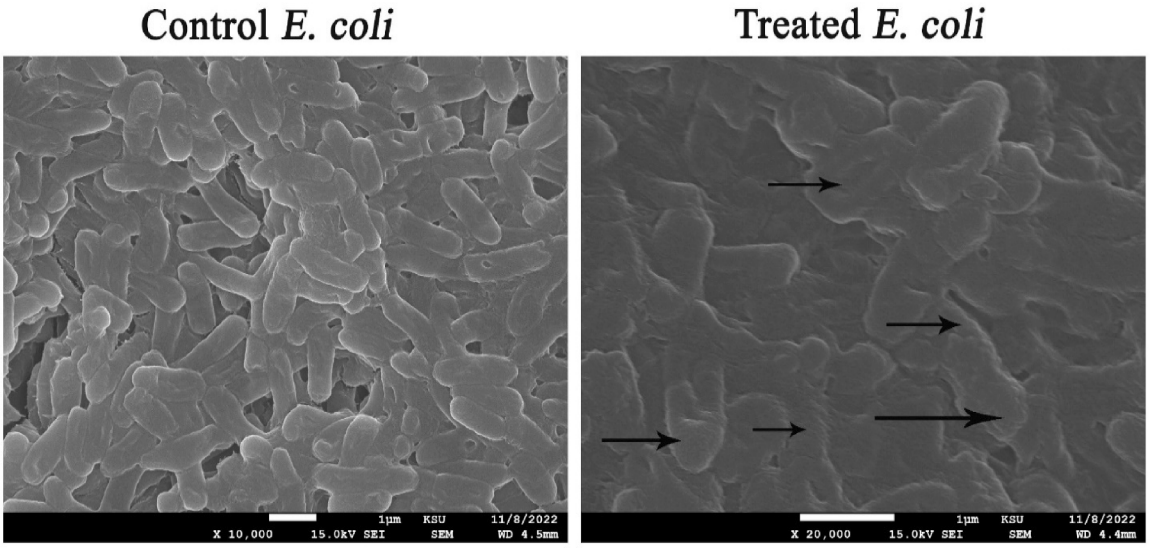


**Fig. 7.** Morphological deformations of *E. coli* cells exposed to biogenic AgNPs (the morphological deformations were pointed out by arrows).

Conceptualization.

## Declaration of competing interest

The authors declare that they have no known competing financial interests or personal relationships that could have appeared to influence the work reported in this paper.

## Acknowledgments

The authors extend their appreciation to the Researchers Supporting Project number (RSP2024R114), King Saud University, Riyadh, Saudi Arabia.

## References

Ahmed, S., Saifullah, A., M., Swami, B.L., Ikram, S.,, 2016. Green synthesis of silver nanoparticles using *Azadirachta indica* aqueous leaf extract. J. Radiat. Res. Appl. Sci. 9, 1–7. https://doi.org/10.1016/j.jrras.2015.06.006.

Ahmed, B., Syed, A., Ali, K., Elgorban, M., A., Khan, A., Lee, J., A. AL-Shwaiman, H.,, 2021. Synthesis of gallotannin capped iron oxide nanoparticles and their broad spectrum biological applications. RSC Adv. 11, 9880–9893. https://doi.org/10.1039/D1RA00220A.

Aljeldah, M.M., Yassin, M.T., Mostafa, A.-A.-F., Aboul-Soud, M.A., 2023. Synergistic Antibacterial Potential of Greenly Synthesized Silver Nanoparticles with Fosfomycin Against Some Nosocomial Bacterial Pathogens. Infect. Drug Resist. 16, 125–142. https://doi.org/10.2147/IDR.S394600.

Almaary, K.S., Yassin, M.T., Elgorban, A.M., Al-Otibi, F.O., Al-Askar, A.A., Maniah, K., 2023. Synergistic antibacterial proficiency of green bioformulated zinc oxide nanoparticles with potential fosfomycin synergism against nosocomial bacterial pathogens. Microorganisms 11 (3), 645.

Al-Otibi, F.O., Yassin, M.T., Al-Askar, A.A., Maniah, K., 2023. Green Biofabrication of Silver Nanoparticles of Potential Synergistic Activity with Antibacterial and Antifungal Agents against Some Nosocomial Pathogens. Microorganisms 11, 945. https://doi.org/10.3390/microorganisms11040945.

Anandalakshmi, K., Venugobal, J., Ramasamy, V., 2016. Characterization of silver nanoparticles by green synthesis method using Pedalium murex leaf extract and their antibacterial activity. Appl. Nanosci. 6, 399–408. https://doi.org/10.1007/s13204-015-0449-z.

Awad, M.A., Hendi, A., A., Ortashi, K.M., Alzahrani, B., Soliman, D., Alanazi, A., Alenazi, W., Taha, R.M., Ramadan, R., El-Tohamy, M., AlMasoud, N., Alomar, T.S.,, 2021. Biogenic synthesis of silver nanoparticles using *Trigonella foenum-graecum* seed extract: Characterization, photocatalytic and antibacterial activities. Sens. Actuators Phys. 323, 112670. https://doi.org/10.1016/j.sna.2021.112670.

Bora, S., Pooja, D., Kulhari, H., 2024. Introduction of Nanoscience and Nanotechnology, in: Pooja, D., Kulhari, H. (Eds.), Nanotechnology Based Delivery of Phytoconstituents and Cosmeceuticals. Springer Nature, Singapore, pp. 1–38. https://doi.org/10.1007/978-981-99-5314-1_1.

Cakić, M., Glišić, S., Cvetković, D., Cvetinov, M., Stanojević, L., Danilović, B., Cakić, K., 2018. Green Synthesis, Characterization and Antimicrobial Activity of Silver Nanoparticles Produced fromFumaria officinalis L. Plant Extract. Colloid J. 80, 803–813. https://doi.org/10.1134/S1061933X18070013.

Calderón-Jiménez, B., Johnson, M.E., Montoro Bustos, A.R., Murphy, K.E., Winchester, M.R., Vega Baudrit, J.R., 2017. Silver Nanoparticles: Technological Advances, Societal Impacts, and Metrological Challenges. Front, Chem, p. 5.

Calzolai, L., Gilliland, D., Rossi, F., 2012. Measuring nanoparticles size distribution in food and consumer products: a review. Food Addit. Contam. Part A 29, 1183–1193. https://doi.org/10.1080/19440049.2012.689777.

Das, B., Dash, S.K., Mandal, D., Ghosh, T., Chattopadhyay, S., Tripathy, S., Das, S., Dey, S.K., Das, D., Roy, S., 2017. Green synthesized silver nanoparticles destroy multidrug resistant bacteria via reactive oxygen species mediated membrane damage. Arab. J. Chem. 10, 862–876. https://doi.org/10.1016/j.arabjc.2015.08.008.

Das, J., Paul Das, M., Velusamy, P., 2013. *Sesbania grandiflora* leaf extract mediated green synthesis of antibacterial silver nanoparticles against selected human pathogens. Spectrochim. Acta. a. Mol. Biomol. Spectrosc. 104, 265–270. https://doi.org/10.1016/j.saa.2012.11.075.

Deivanathan, S.K., Prakash, J.T.J., 2022. Green synthesis of silver nanoparticles using aqueous leaf extract of *Guettarda Speciosa and its* antimicrobial and anti-oxidative properties. Chem. Data Collect. 38, 100831. https://doi.org/10.1016/j.cdc.2022.100831.

Dhaka, A., Chand Mali, S., Sharma, S., Trivedi, R., 2023. A review on biological synthesis of silver nanoparticles and their potential applications. Results Chem. 6, 101108. https://doi.org/10.1016/j.rechem.2023.101108.

Gomathi, M., Rajkumar, P.V., Prakasam, A., Ravichandran, K., 2017. Green synthesis of silver nanoparticles using *Datura stramonium* leaf extract and assessment of their antibacterial activity. Resour.-Effic. Technol. 3, 280–284. https://doi.org/10.1016/j.reffit.2016.12.005.

Hajebi, S., Tabrizi, M.H., Moghaddam, M.N., Shahraki, F., Yadamani, S., 2019. Rapeseed flower pollen bio-green synthesized silver nanoparticles: a promising antioxidant, anticancer and antiangiogenic compound. JBIC J. Biol. Inorg. Chem. 24, 395–404. https://doi.org/10.1007/s00775-019-01655-4.

Hamad, A., Khashan, K.S., Hadi, A., 2020. Silver Nanoparticles and Silver Ions as Potential Antibacterial Agents. J. Inorg. Organomet. Polym. Mater. 30, 4811–4828. https://doi.org/10.1007/s10904-020-01744-x.

Huang, M., Ma, Y., Qian, J., Sokolova, I.M., Zhang, C., Waiho, K., Fang, J.K.H., Ma, X., Wang, Y., Hu, M., 2024. Combined effects of norfloxacin and polystyrene nanoparticles on the oxidative stress and gut health of the juvenile horseshoe crab *Tachypleus tridentatus*. J. Hazard. Mater. 468, 133801. https://doi.org/10.1016/j.jhazmat.2024.133801.

Jalilian, F., Chahardoli, A., Sadrjavadi, K., Fattahi, A., Shokoohinia, Y., 2020. Green synthesized silver nanoparticle from *Allium ampeloprasum* aqueous extract: Characterization, antioxidant activities, antibacterial and cytotoxicity effects. Adv. Powder Technol. 31, 1323–1332. https://doi.org/10.1016/j.apt.2020.01.011.

Jeevanandam, J., Kiew, S.F., Boakye-Ansah, S., Lau, S.Y., Barhoum, A., Danquah, M.K., Rodrigues, J., 2022. Green approaches for the synthesis of metal and metal oxide nanoparticles using microbial and plant extracts. Nanoscale 14, 2534–2571.

Kakakhel, M.A., Sajjad, W., Wu, F., Bibi, N., Shah, K., Yali, Z., Wang, W., 2021. Green synthesis of silver nanoparticles and their shortcomings, animal blood a potential source for silver nanoparticles: A review. J. Hazard. Mater. Adv. 1, 100005. https://doi.org/10.1016/j.hazadv.2021.100005.

Kathiravan, V., Ravi, S., Ashokkumar, S., Velmurugan, S., Elumalai, K., Khatiwada, C.P., 2015. Green synthesis of silver nanoparticles using *Croton sparsiflorus morong* leaf extract and their antibacterial and antifungal activities. Spectrochim. Acta. a. Mol. Biomol. Spectrosc. 139, 200–205. https://doi.org/10.1016/j.saa.2014.12.022.

Khalil, M.M.H., Ismail, E.H., El-Baghdady, K.Z., Mohamed, D., 2014. Green synthesis of silver nanoparticles using olive leaf extract and its antibacterial activity. Arab. J. Chem. 7, 1131–1139. https://doi.org/10.1016/j.arabjc.2013.04.007.

Kumar, V., Singh, S., Srivastava, B., Bhadouria, R., Singh, R., 2019. Green synthesis of silver nanoparticles using leaf extract of Holoptelea integrifolia and preliminary investigation of its antioxidant, anti-inflammatory, antidiabetic and antibacterial activities. J. Environ. Chem. Eng. 7, 103094. https://doi.org/10.1016/j.jece.2019.103094.

Mistry, H., Thakor, R., Patil, C., Trivedi, J., Bariya, H., 2021. Biogenically proficient synthesis and characterization of silver nanoparticles employing marine procured fungi Aspergillus brunneoviolaceus along with their antibacterial and antioxidative potency. Biotechnol. Lett. 43, 307–316. https://doi.org/10.1007/s10529-020-03008-7.

Muenraya, P., Sawatdee, S., Srichana, T., Atipairin, A., 2022. Silver Nanoparticles Conjugated with Colistin Enhanced the Antimicrobial Activity against Gram-Negative Bacteria. Molecules 27, 5780. https://doi.org/10.3390/molecules27185780.

Naaz, R., Siddiqui, V.U., Qadir, S.U., Siddiqi, W.A., 2021. Green synthesis of silver nanoparticles using *Syngonium podophyllum* leaf extract and its antibacterial activity. Mater. Today Proc., ICMN-2020 46, 2352–2358. https://doi.org/10.1016/j.matpr.2021.05.062.

Nie, P., Zhao, Y., Xu, H., 2023. Synthesis, applications, toxicity and toxicity mechanisms of silver nanoparticles: A review. Ecotoxicol. Environ. Saf. 253, 114636. https://doi.org/10.1016/j.ecoenv.2023.114636.

Oves, M., Ahmar Rauf, M., Aslam, M., Qari, H.A., Sonbol, H., Ahmad, I., Sarwar Zaman, G., Saeed, M., 2022. Green synthesis of silver nanoparticles by Conocarpus Lancifolius plant extract and their antimicrobial and anticancer activities. Saudi J. Biol. Sci. 29, 460–471. https://doi.org/10.1016/j.sjbs.2021.09.007.

Paosen, S., Saising, J., Wira Septama, A., Piyawan Voravuthikunchai, S., 2017. Green synthesis of silver nanoparticles using plants from Myrtaceae family and characterization of their antibacterial activity. Mater. Lett. 209, 201–206. https://doi.org/10.1016/j.matlet.2017.07.102.

Paulkumar, K., Gnanajobitha, G., Vanaja, M., Rajeshkumar, S., Malarkodi, C., Pandian, K., Annadurai, G., 2014. Piper nigrum Leaf and Stem Assisted Green Synthesis of Silver Nanoparticles and Evaluation of Its Antibacterial Activity Against Agricultural Plant Pathogens. Sci. World J. 2014, 829894. https://doi.org/10.1155/2014/829894.

Polash, S.A., Hossain, M.M., Saha, T., Sarker, S.R., 2021. Biogenic Silver Nanoparticles: A Potent Therapeutic Agent. In: Singh, S. (Ed.), Emerging Trends in Nanomedicine. Springer, Singapore, pp. 81–127. https://doi.org/10.1007/978-981-15-9920-0_4.

Raghava, S., Munnene Mbae, K., Umesha, S., 2021. Green synthesis of silver nanoparticles by *Rivina humilis* leaf extract to tackle growth of *Brucella* species and other perilous pathogens. Saudi J. Biol. Sci. 28, 495–503. https://doi.org/10.1016/j.sjbs.2020.10.034.

Ramalingam, B., Parandhaman, T., Das, S.K., 2016. Antibacterial Effects of Biosynthesized Silver Nanoparticles on Surface Ultrastructure and Nanomechanical Properties of Gram-Negative Bacteria viz. *Escherichia coli* and *Pseudomonas aeruginosa*. ACS Appl. Mater. Interfaces 8, 4963–4976. https://doi.org/10.1021/acsami.6b00161.

Restrepo, C.V., Villa, C.C., 2021. Synthesis of silver nanoparticles, influence of capping agents, and dependence on size and shape: A review. Environ. Nanotechnol. Monit. Manag. 15, 100428.

Rizwana, H., Alwhibi, M.S., Al-Judaie, R.A., Aldehaish, H.A., Alsaggabi, N.S., 2022. Sunlight-mediated green synthesis of silver nanoparticles using the berries of Ribes rubrum (red currants): Characterisation and evaluation of their antifungal and antibacterial activities. Molecules 27, 2186.

Roy, A., Bulut, O., Some, S., Mandal, A.K., Yilmaz, M.D., 2019. Green synthesis of silver nanoparticles: biomolecule-nanoparticle organizations targeting antimicrobial activity. RSC Adv. 9, 2673–2702.

Sharma, A., Sagar, A., Rana, J., Rani, R., 2022. Green synthesis of silver nanoparticles and its antibacterial activity using fungus Talaromyces purpureogenus isolated from

Taxus baccata Linn. Micro Nano Syst. Lett. 10, 2. https://doi.org/10.1186/s40486-022-00144-9.

Shnoudeh, A.J., Hamad, I., Abdo, R.W., Qadumii, L., Jaber, A.Y., Surchi, H.S., Alkelany, S.Z., 2019. Chapter 15 - Synthesis, Characterization, and Applications of Metal Nanoparticles. In: Tekade, R.K. (Ed.), Biomaterials and Bionanotechnology, Advances in Pharmaceutical Product Development and Research. Academic Press, pp. 527–612. https://doi.org/10.1016/B978-0-12-814427-5.00015-9.

Syafiuddin, A., Salmiati, S., M.R., Beng Hong Kueh, A., Hadibarata, T., Nur, H.,, 2017b. A Review of Silver Nanoparticles: Research Trends, Global Consumption, Synthesis, Properties, and Future Challenges. J. Chin. Chem. Soc. 64, 732–756. https://doi.org/10.1002/jccs.201700067.

Syafiuddin, A., Salmiati, H., T., Salim, M.R., Kueh, A.B.H., Sari, A.A.,, 2017a. A purely green synthesis of silver nanoparticles using Carica papaya, Manihot esculenta, and Morinda citrifolia: synthesis and antibacterial evaluations. Bioprocess Biosyst. Eng. 40, 1349–1361. https://doi.org/10.1007/s00449-017-1793-z.

Tavares, T.D., Antunes, J.C., Padrão, J., Ribeiro, A.I., Zille, A., Amorim, M.T.P., Ferreira, F., Felgueiras, H.P., 2020. Activity of specialized biomolecules against gram-positive and gram-negative bacteria. Antibiotics 9, 314.

Tripathi, N., Goshisht, M.K., 2022. Recent Advances and Mechanistic Insights into Antibacterial Activity, Antibiofilm Activity, and Cytotoxicity of Silver Nanoparticles. ACS Appl. Bio Mater. 5, 1391–1463. https://doi.org/10.1021/acsabm.2c00014.

Varghese, R., Almalki, M.A., Ilavenil, S., Rebecca, J., Choi, K.C., 2019. Silver nanopaticles synthesized using the seed extract of *Trigonella foenum-graecum* L. and their antimicrobial mechanism and anticancer properties. Saudi J. Biol. Sci. 26, 148–154. https://doi.org/10.1016/j.sjbs.2017.07.001.

Wang, F., Zhang, W., Tan, X., Wang, Z., Li, Y., Li, W., 2019. Extract of *Ginkgo biloba* leaves mediated biosynthesis of catalytically active and recyclable silver nanoparticles. Colloids Surf. Physicochem. Eng. Asp. 563, 31–36. https://doi.org/10.1016/j.colsurfa.2018.11.054.

Yassin, M.T., Mostafa, A.-A.-F., Al-Askar, A.A., Al-Otibi, F.O., 2022a. Synergistic Antibacterial Activity of Green Synthesized Silver Nanomaterials with Colistin Antibiotic against Multidrug-Resistant Bacterial Pathogens. Crystals 12, 1057. https://doi.org/10.3390/cryst12081057.

Yassin, M.T., Mostafa, A.-A.-F., Al-Askar, A.A., Al-Otibi, F.O., 2022b. Facile Green Synthesis of Silver Nanoparticles Using Aqueous Leaf Extract of Origanum majorana with Potential Bioactivity against Multidrug Resistant Bacterial Strains. Crystals 12, 603. https://doi.org/10.3390/cryst12050603.

Yassin, M.T., Mostafa, A.-A.-F., Al-Askar, A.A., Al-Otibi, F.O., 2022c. Synergistic Antifungal Efficiency of Biogenic Silver Nanoparticles with Itraconazole against Multidrug-Resistant Candidal Strains. Crystals 12, 816. https://doi.org/10.3390/cryst12060816.

Yassin, M.T., Al-Otibi, F.O., Al-Askar, A.A., Alharbi, R.I., 2023. Green Synthesis, Characterization, and Antifungal Efficiency of Biogenic Iron Oxide Nanoparticles. Appl. Sci. 13, 9942. https://doi.org/10.3390/app13179942.